Xu, L.; Willumeit-Römer, R.; Luthringer-Feyerabend, B.:

Mesenchymal Stem Cell and Oxygen Modulate the Cocultured Endothelial Cells in the Presence of Magnesium Degradation Products.

In: ACS Applied Bio Materials. Vol. 4 (2021) 3, 2398 - 2407.

First published online by ACS: 26.02.2021.

https://dx.doi.org/10.1021/acsabm.0c01289

Mesenchymal Stem Cell and Oxygen Modulate the Cocultured Endothelial Cells in the Presence of Magnesium Degradation Products

Lei Xu, Regine Willumeit-Römer, and Bérengère J. C. Luthringer-Feyerabend*

ABSTRACT: The interaction between mesenchymal stem cells (MSCs) and endothelial cells (ECs) holds a promising potential for the revascularization of osteoconductive grafts in orthopedics regeneration. Magnesium (Mg), as a well studied degradable biomaterial already used in current medical practice, possesses osteoinductive properties. We investigated whether the physi ochemical microenvironment, that is, the Mg and oxygen contents, further influences the MSC modulating EC activities. Hypoxia, normoxia, and Mg degradation were represented by 5 and 20% O_2 and gradient Mg degradation products, respectively. The migration of ECs in both EC mono and MSC−EC coculture was increased in Mg with normoxia. Tube formation of ECs was reduced by Mg, especially in coculture and under normoxia. Compared to the monoculture, MSC−EC coculture exhibited significantly decreased content of proangiogenic cytokines but an increased amount of chemotactic factors. Semiquantitative real time polymerase chain reaction revealed significant different profiles of the gene regulation under hypoxia, normoxia, different cell populations, and cell status. Investigation of heterotypic MSC−EC interactions in a mixed coculture system exhibited significantly increased proliferation under hypoxia. Transdifferentiation between MSCs and ECs was found to be reciprocally regulated by Mg degradation products in the two different oxygen conditions, probably because of the variable regulating effects of Mg on hypoxia inducible factors. These results indicated the modulatory roles of oxygen tension and MSCs in combination with Mg or Mg based degradable materials.

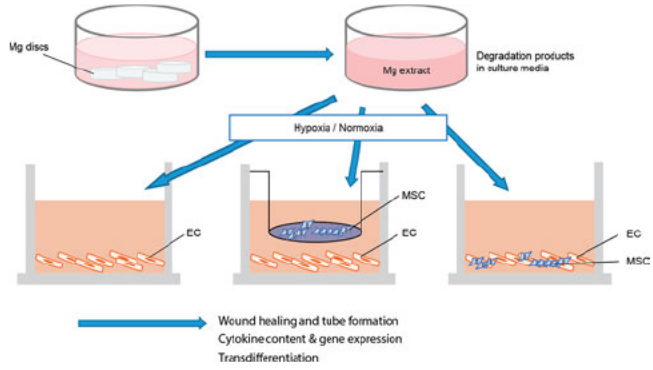

INTRODUCTION

Magnesium (Mg) based biomaterials belong to the "smart" materials, combining biodegradability and bioactivity (even eliciting specific cellular responses at the molecular level).[1] With suitable (*e.g.,*) alloying and processing strategies, degradation rates as well as mechanical properties can nowadays be tailored, allowing for various biological applications. The two main clinical applications are targeting the musculoskeletal [Magnezix compression screw; Syntellix AG, Hanover, Germany—Resomet (K MET) screw; U&I Corporation, Seoul, Republic of Korea] and cardiovascular (Magmaris scaffold; Biotronik AG, Bülach, Switzerland) systems. However, the use of Mg based biomaterials is a growing field of application (*e.g.*, neural electrodes,[2] nerve guidance conduits,[3] and cancer therapy[4]). Nevertheless, independent of the application type, tissue or wound healing is a repairing process that happens after implantation. During the proliferative phase, angiogenesis or neovascularization is the formation of new blood capillaries and the prerequisite for tissue reconstitution by providing circulating oxygen, mole cules (nutrients, water, and ions), and stem cells. Angiogenesis is a regulated process involving the proliferation, migration, and remodeling of endothelial cells (ECs) from adjacent pre existing blood vessels. Concomitantly, stem cells are recruited at the injury site from the adjacent tissue and out of the circulation.[5] Mesenchymal stem cells (MSCs) are widely available from birth related tissues and with high and rather stable *in vitro* expansion capacity. MSCs are proved to modulate angiogenesis *via* their paracrine secretion of tropic factors.[6] The interplay between MSCs and ECs is a promising strategy for enhancing the revascularization during tissue repair, especially in regenerative orthopaedics.[7,8] The pro liferation and permeability of ECs can be influenced by the basic fibroblast growth factor (bFGF),[9] interleukin 8 (IL8),[10]

bone morphogenetic protein (BMP) signaling,[11] matrix metalloproteinases (MMPs),[12] and tissue inhibitor of metal loproteinase 1 (TIMP1).[13] Angiogenic effects of an MSC are mediated by the vascular endothelial growth factor (VEGF)[14] and platelet derived growth factor (PDGF).[15] Besides the communication *via* cytokines, emerging results suggest that the heterotypic contact may promote cellular transdifferentia tion.[16] In other words, transdifferentiated ECs from MSCs could be beneficial for the growth and differentiation of the EC.[17,18]

Effects of Mg deficiency (in opposition to increased physiological Mg concentrations) on an endothelial system have been mostly studied *in vitro* and *in vivo* and highlighted its dysfunctions. *In vitro*, Mg deficiency resulted in altered proliferation and migration, accompanied by a nuclear factor k B (NF kB) pathway activation, increased levels of IL8, IL6, IL1, tumor necrosis factor α (TNFα), reactive oxygen species (ROS), prostaglandin E2 (PGE2), and nitric oxide synthase (NOS) activity.[19−23] *In vivo*, contradictory Mg supplementa tion effects were observed. However, the systematic review and meta analysis of randomized controlled Mg supplementation on endothelial function trials performed by Darooghegi Mofrad *et al.*[24] highlighted that daily supplementation of Mg had a significant effect (increase) on flow mediated dilation.

Mg based materials are promising biomaterials for vascula rization related therapies; thanks to their mechanical properties and biocompatibility. Mg degradation products have proved to improve *in vivo* vascularization and *in vitro* endothelial migration and proliferation[25,26] and the activities of MSCs.[27−30] Besides impacting the implant's mechanical properties, the degradation of Mg in body fluids or *in vitro* aqueous environments could ultimately modify local oxygen concentration as Mg degradation consummates dissolved oxygen.[31] The local oxygen content is decisive for proper vascularization and MSC's fate. For instance, hypoxia increases oxidative stress and endothelial activation.[29] Oxygen can influence the differentiation and multipotent status or tropic secretion of MSCs.[30] Oxygen tension varies from tissue sites (about 6% in bone marrow and 4−14% in the vascularized system[32,33]), health status, and healing phases like the usual hypoxic condition during tissue healing neovascularization (about 4% in adult mice tibial fractures[34]). Furthermore, 5% O_2 was selected in many hypoxia research studies;[35−37] thus we choose 5 and 20% to represent hypoxia and normoxia, respectively. A previous study of EC monoculture[25] indicated that increased Mg concentrations had a general negative effect on early (migration) and late (tubulogenesis) angiogenesis under normoxia. However, under hypoxia, these effects were absent. The interplay between oxygen content Mg or even degradable materials and the MSC and EC interactions, two important constituents of bone marrow, represent high scientific interest for tissue engineering and biodegradable Mg applications and remain to be fully understood. Therefore, with special interest in orthopedic applications, we mimic the effects of Mg degradation and oxygen content on the vascularization of EC and MSC−EC interactions using monoculture and coculture systems as well as different concentrations of Mg degradation products and oxygen contents. We applied cell culture medium containing 0.813 mM Mg as the physiological level of Mg in blood (control) and 2, 4, and 8 mM Mg containing degradation products because up to 10 mM has no adverse effects on ECs.[30]

MATERIALS AND METHODS

Coculture Models and Settings. The migration and morpho genesis are two essential steps during angiogenesis. Previous studies of EC monoculture indicates the significant effects of Mg degradation products and oxygen tension on these two angiogenic stages.[20] In order to investigate the roles of MSCs, we set up three cell culture models (Table 1) and compared the obtained results to the ones of the former EC monoculture. First, to induce the migration and morphogenesis of ECs, transwell coculture was applied. Especially, a thin layer angiogenesis (TLA) assay was used to examine tube formation (morphogenesis) of ECs, allowing for quantitative real time polymerase chain reaction and microscopy studies.[38] In addition, a cell mixture coculture was applied to represent the latter stage of MSC−EC interaction, in which the proliferation and cellular transdifferentiation were investigated.

Table 1. Models of Monoculture and Coculture

model	component	methodology
monoculture	EC	wound healing
		tube formation
transwell coculture	MSCs and ECs separated by transwell	wound healing
		tube formation
direct coculture	mixture of MSCs and ECs	proliferation
		transdifferentiation

Isolation and Immunophenotyping of MSCs and ECs. Cell isolation's ethical approval was acquired from the Ethics Committee of the Hamburg Medical Association (PV4058). MSCs were isolated from Wharton's jelly of arteries and thus also termed human umbilical perivascular cells (HUCPV). The detailed isolation protocol can be found here.[39] MSCs were expanded in minimum essential medium eagle α modification (α MEM, Fisher Scientific GmbH, Schwerte, Germany) supplemented with 15% fetal bovine serum optimized for human MSCs (SC FBS, Biological Industries, Beit Haemek, Israel) and 1% penicillin streptomycin (P/S, Fisher Scientific GmbH, Schwerte, Germany). ECs were derived from the lumen of an umbilical vein using collagenases, type IA (Sigma Aldrich Chemie GmbH, Taufkirchen, Germany). The complete isolation procedure was previously published by Xu *et al.*[25] The proper identities of MSCs and ECs were validated by their immunophenotyping with flow cytometry using a cell specific cluster of differentiation (Supporting Information S2: antibodies and isotype controls selected for flow cytometry—results can be found here[40]). HUVEC and HUCPV (up to passage 6th and 12th, respectively) were used.

Magnesium Degradation Products. After permanent mold gravity casting, pure Mg (99.95%) ingots were T4 treated and extruded into rods (Ø 1 cm; Helmholtz Zentrum Geesthacht, Geesthacht, Germany). Subsequently, discs were prepared (1.5 mm thickness) from the further machined rods (Ø 0.9 cm). The discs were sonically cleaned (100% *n* hexane, acetone, and ethanol for 20 min), sterilized with ethanol (70%, for 20 min; Merck, Darmstadt, Germany), and finally sterilely air dried. Extracts obtained from the Mg sample degradation were obtained following EN ISO standards I. 10993 5:2009 and I. 10993 12:2012 (*i.e.*, 0.2 g Mg in 1 mL extraction medium, here α MEM supplemented with 15% SC FBS and 1% P/S) under cell culture conditions for 72 h. The extract Mg content was measured *via* inductively coupled plasma mass spectrometry (ICP−MS; Agilent, Waldbron, Germany). The degradation products containing solutions were prepared by diluting Mg degradation extract into 2/4/8 mM Mg with α MEM supplemented with 15% SC FBS and 1% P/S. The osmolality (measured with a cryoscopic osmometer; Gonotec, Berlin, Germany) and pH (Sentron pH Meter; Sentron Europe BV, VD Leek, Netherlands) were investigated and found to be not significantly different compared to cell culture medium.

Monoculture and Transwell Coculture. *Wound Healing Assay.* The wound healing assay was performed to elucidate the

cellular edge extension during the migration of ECs. The ECs were maintained in 1.5 mL of endothelial cell growth medium (ECGM, PromoCell, Heidelberg, Germany) plus FBS (Biochrom, Berlin, Germany) until approaching 80% confluence. MSCs were seeded in 1.5 mL of α MEM supplemented with 15% SC FBS and 1% P/S (same as extraction medium). Before wound healing assay, ECs were starved in ECGM with 1% FBS for 24 h to obtain a synchronized cellular cycle. Prior to wound healing assay, ECs were treated with mitomycin C (10 μg/mL) to inhibit proliferation for 2 h. MSCs (80,000 cells, in the inserts and ECs (20,000 cells, at the bottom chamber) per well) were seeded in 24 well plates. Wounds of the EC were produced using a 1 mL pipette tip on the cell monolayer at 0 h (Supporting Information S3). Wounds were cultured in Mg degradation products under 20 and 5% O_2 for 24 h. Hypoxia was achieved by replacing oxygen by nitrogen in an incubator with an oxygen sensor (Thermo Scientific—Fisher Scientific GmbH, Langenselbold, Germany), an efficient method to provide stable conditions.[41] Acquisition of the pictures was performed at 0 h (T0) and after 24 h (T24) with a Ti S/L100 microscope (Nikon GmbH, Dusseldorf, Germany). The cellular edge extension was calculated from the scratch difference between T0 and T24 using Image Processing and Analysis in Java (ImageJ version 1.51b; National Institutes of Health, Bethesda, USA) with the MRI plugin. The supernatants and cells were collected and stored at −80 °C for further experiments.

Tube Formation Assay. An adapted thin layer assay (TLA)[38] was applied. MSCs and ECs were maintained, as described in the wound healing assay. The matrix (Geltrex, Fisher Scientific GmbH, Schwerte, Germany) was homogeneously spread with a pipette tip on each well bottom of 24 well plates. The coating was polymerized at 37 °C for 30 min. MSCs were seeded in the inserts (80,000 cells). ECs were seeded as 4000 cells per reconstituted matrix layer in bottom chambers of 24 well plates. The image was visualized using an inverted microscope at 6 h. The number of branches and the total length of the tubes were quantified by ImageJ with an Angiogenesis Analyzer Plugin (Gilles Carpentier Research). The supernatants and cells were collected and stored at −80 °C for further experiments.

Direct Coculture. *Transdifferentiation Assessment.* MSCs and ECs (200,000:50,000 cells) were seeded in T25 flasks for 7 days. The medium was refreshed every 3 days. On days 1, 4, and 7, supernatants and cells were collected and stored at −80 °C for further experiments. The CD 90 (Thy 1 cell surface antigen) and CD 31 (platelet EC adhesion molecule 1) in total cell population were measured using flow cytometry on days 1, 4, and 7. The cell dissociation was performed using trypsin−EDTA (0.05%; Thermo Scientific—Fisher Scientific GmbH, Langenselbold, Germany), adjusted to 500,000 cells in 20 μL of staining buffer, and stained with the antibody solutions. Cells resuspended in phosphate buffered saline (PBS) served as a blank control. The bovine serum albumin in PBS (1% w/v) was used as the staining buffer. Samples were incubated with antibodies on ice for 30 min in darkness. Stained cells were washed once with warm staining buffer. Cells were resuspended in a 5 mL of ice cold PBS. Total 5000 events per measurement were collected with a Flow cytometer S3e (Bio Rad Laboratories GmbH, Munich, Germany) using ProSortTM software (v1.5; Bio Rad Laboratories GmbH, Munich, Germany). Ultimately, the results were quantified using Flow Jo (version 10.5.3; Ashland, Oregon, USA) by removing debris events, death population (positive propidium iodide staining). The population was double stained by CD 90 and 31 were compensated with their single staining.

Proliferation. In order to assess cells' metabolic activity or cell proliferation, WST 1 assay was performed. ECs and MSCs were seeded as 4:1 (5000 cells in total) *per* well in 96 well plates at 37 °C for 1, 4, and 7 days. Every 3 days, the media was renewed (0.4 mL). At day 1, 4, and 7, the media was exchanged with 0.2 mL of fresh α MEM complete medium supplemented with 20 μL of WST 1 (Takara Bio Inc., Shiga, Japan) for 30 min in 37 °C. The optical absorbance of 100 μL of each sample was measured at 450 nm using a Sunrise microplate reader (TECAN Deutschland GmbH, Crailsheim, Germany). Afterward, DNA content was measured using bisbenzimide (Sigma Aldrich Chemie GmbH, Munich, Germany) in order to normalize the variation induced by cell proliferation. In parallel, at day 1, 4, and 7 cells were stained with rhodamine 123 (10 μg/mL in PBS, Sigma Aldrich, Munich, Germany) and 4′,6 diamidino 2 phenylindole (1 μg/mL DAPI in ddH_2O; Sigma Aldrich, Munich, Germany).

Enzyme-Linked Immunosorbent Assay. Supernatants were thawed on ice and centrifuged at 2000 rpm for 2 min. Expression of IL8, platelet derived growth factor subunit A (PDGFA), metalloproteinase inhibitor 1 (TIMP1), fibroblast growth factor 2 (bFGF), and transforming growth factor β 1 (TGFb1) were measured *via* enzyme linked immunosorbent assay (ELISA). All ELISAs were purchased from R&D (R&D Systems GmbH, Wiesbaden, Germany) and prepared according to manufacturer instructions. The capture antibody was coated in 96 well plates 50 μL per well for 12 h at room temperature (RT). The plates were blocked with 50 μL of block buffer for 1 h at RT. Samples (or standards) were bound with 50 μL of capture antibodies for 1 h at RT. Detection antibodies were added to plates 50 μL per well for 1 h at RT. Streptavidin−horseradish peroxidase (HRP) was added to detection antibodies for 20 min at RT avoiding direct light. Plates were incubated for 20 min with 50 μL of substrate solution at RT with no direct light. The reaction was terminated with 25 μL of stop solution (corrosive sulfuric acid) and measured with a Sunrise microplate reader (TECAN Deutschland GmbH, Crailsheim, Germany) at 450 nm (540 nm as reference wavelength). Between each coating and reaction, plates were washed 2 times with 150 μL of washing buffer using a Bio Plex Pro wash station (Bio Rad Laboratories GmbH, Munich, Germany). Cytokine concentrations were quantified with standard curves.

Real-Time Quantitative Polymerase Chain Reaction. Total ribonucleic acid (RNA) was extracted using QIAshredder and RNeasy kit (QIAGEN GmbH, Hilden, Germany). The RNA concentration [optical density (OD) at 260 nm] and purity (OD at 260/280 nm) were measured using a NanoDrop spectrophotometer (Thermo Scientific—Fisher Scientific GmbH, Schwerte, Germany). Complementary deoxyribonucleic acid (cDNA) was synthesized *via* reverse transcription using a reverse transcription Kit Omniscript from QIAGEN GmbH (Hilden, Germany). Primers (either selected from the RTPrimerDB database or prepared *via* Primer 3; version 4.0.0) were purchased from Eurofins GmbH (Hamburg, Germany). Actin β (*ACTB*) and glyceraldehyde 3 phosphate dehydrogenase (*GAPDH*) were selected as reference genes. All primers are presented in Supporting Information S4. RT qPCR was achieved using SsoFast EvaGreen Supermix with a PCR detection system (CFX96 Touch) and CFX Manager Software (Bio Rad Laboratories GmbH, Munich, Germany). The thermal cycling conditions included (i) an initial denaturation at 95 °C for 3 min, (ii) 40 cycles of denaturation (20 s at 95 °C), annealing (20 s at 60 °C), and elongation (30 s at 75 °C), (iii) and a melting curve step (30 s at 95 °C and then heating from 65 to 95 with 0.5 °C increments of 5 s). Control without cDNA or "no treatment control" was included.

Statistical Analysis. Two independent experiments with two technical replicates, using cells of three donors (n = 12), were performed. The statistical differences between control and Mg treatment were analyzed with one way ANOVA following Dunnett's post hoc multiple comparisons (α = 0.05) *via* SigmaPlot version 13.0 (Systat software GmbH, Erkrath, Germany). The comparison between oxygen at the same Mg treatment was analyzed with a paired t test (α = 0.05) using SigmaPlot. In RT qPCR, t test (with α = 0.05) was performed, and differential expressions were calculated *via* CFX manager software (V3.1; Bio Rad, Munich, Germany).

RESULTS

Monoculture and Transwell Coculture. *Wound Healing and Tube Formation of ECs.* Wound closure was calculated from the scratch areas between the T0 and T24 (0 and 24 h)—see Figure 1. Scratches at T0 made the unified noncell area for further comparison at T24. As our previous work indicated, Mg degradation products had no influence under 5% O_2.[25] However, at 20% O_2, an increased closure area

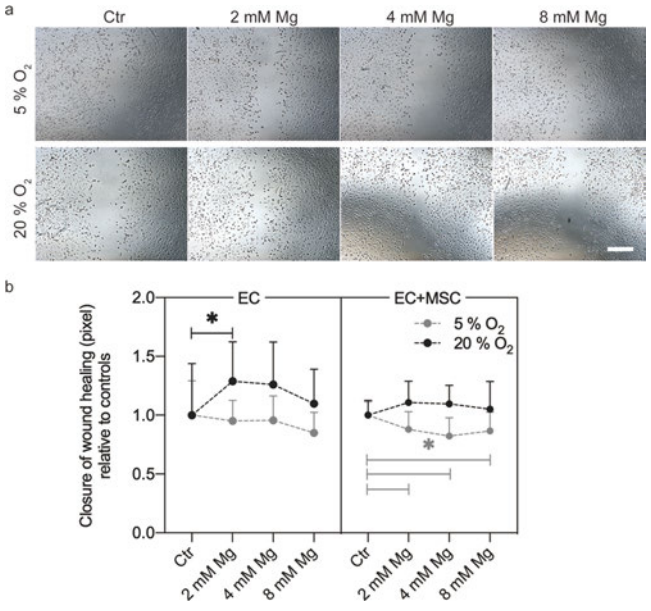

Figure 1. Wound healing: assessment of EC migration in monoculture and transwell coculture. Data were collected from two technical replicates of two independent experiments from cells of three donors (n = 12). (a) Pictures were acquired with an inverted microscope at 0 and after 24 h. Here, exemplary pictures of EC cocultured with MSCs after 24 h (starting migration at T0 can be found in Figure S1) are presented. Scale bar represents 500 μm. (b) No cell area difference between T0 and T24 of EC monoculture and coculture with MSCs was quantified using ImageJ. Data are represented as arithmetic mean ± standard deviation. Significances between Mg treatments and controls were tested by ANOVA and indicated by an asterisk (α = 0.05, $^{*}P \leq 0.05$).

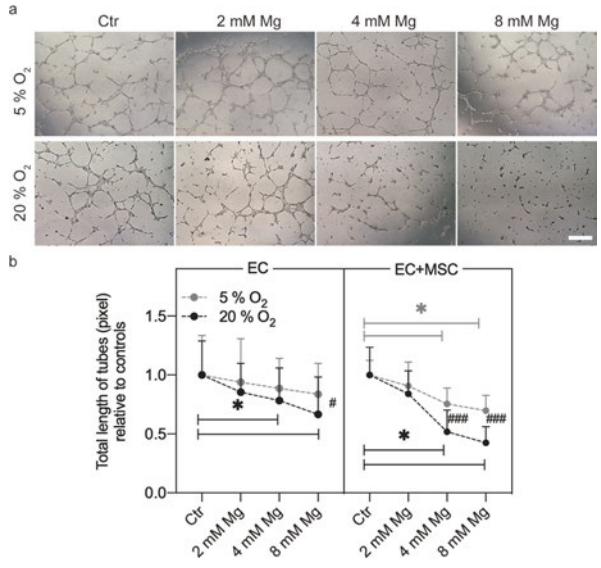

Figure 2. Tube formation of ECs in monoculture and transwell coculture. Data were collected from 2 technical replicates of two independent experiments from cells of three donors (n = 12). (a) Pictures were acquired with an inverted microscope at the 6th h (representative pictures are presented); scale bar represents 500 μm. (b) Total length of tubes of EC monoculture and coculture with MSCs was quantified using ImageJ. Data are represented as arithmetic mean ± standard deviation. Significances between Mg treatments and controls were tested by ANOVA and indicated by an asterisk (α = 0.05, $^{*}P \leq 0.05$). Significance between 5 and 20% O_2 within same Mg treatments was tested by paired t test and indicated by hashtags (α = 0.05, $^{\#}P \leq 0.05$, and $^{\#\#\#}P \leq 0.001$).

of EC monoculture was observed in EC monoculture (statistical difference with 2 mM Mg). When cocultured with MSCs at 20% O_2, Mg concentrations had no effects on migration. Conversely, at 5% O_2, EC migration in coculture was inhibited by increased Mg concentrations.

Tube formation was acquired from the tube formation areas after 6 h and the total length was quantified (Figure 2). Under 5% O_2, the total length of tubes in EC monoculture was not remarkably changed after 6 h. However, at 20% O_2, the total length was clearly reduced by 4 and 8 mM Mg (Figure 2b).[20] When cocultured with MSCs, the total length of ECs was decreased significantly by 4 and 8 mM Mg at both 5 and 20% O_2.

Cytokine Expression in Wound Healing and Tube Formation. By merging the different Mg treatments and mono /coculture conditions, results emphasized no significant difference between high and low oxygen (Figure 3a—left). However, all cytokines especially PDGFA, TIMP1, and bFGF were significantly decreased when ECs were cocultured with MSCs (Figure 3a—right). In the wound healing of EC monoculture (Figure 3b), 8 mM Mg significantly decreased PDGFA at 5% O_2. At 20% O_2, TIMP1 was significantly decreased with 8 mM Mg. IL8 was remarkably increased at both 5 and 20% O_2 with 4 or 8 mM Mg. Similar results were also observed for bFGF (except for 5% 4 mM Mg). Within cocultures, a general decrease of PDGFA, TIMP1, and bFGF productions was observed with increasing concentrations of Mg (except for the expression of bFGF, which remained constant at 5% O_2 and TIMP1 production which was significantly decreased only by 2 mM Mg at 5% O_2). Especially at 20% O_2, PDGFA was significantly decreased with up to 8 mM Mg, whereas TIMP1 was significantly decreased by 4 and 8 mM Mg. Under 5% O_2, PDGFA was significantly reduced by 8 mM Mg. The bFGF level in coculture was significantly reduced with 8 mM Mg at 20% O_2. However, the level of IL8 was only increased by 8 mM Mg at 20% O_2.

By considering the effect of oxygen content on tube formation (Figure 4a—right), all cytokines except for PDGFA were significantly upregulated when ECs were cocultured with MSCs. In the tube formation of EC monoculture, a decrease of IL8 and bFGF was found with 2 and 4 mM Mg under 5% O_2, respectively. Under 20% O_2, only bFGF content was significantly decreased with all Mg concentrations. In the cocultures, both PDGFA and TIMP1 contents were significantly reduced with increasing concen tration of Mg under 20% O_2. Under 5% O_2, PDGFA remained constant. TIMP1 and bFGF contents decreased with Mg (statistically for all Mg concentrations for TIMP1 and only for 8 mM for bFGF). However, for IL8 an increased expression could be observed (statistically with 8 mM Mg).

Gene Expression in Wound Healing and Tube Formation. During the wound healing and tube formation of the EC, the gene expressions of MSCs (upper insert) and ECs (bottom chamber) in transwell were investigated (Figure 5). Under 5% O_2 in ECs, angiogenin (*ANG*), *IL8*, and vascular endothelial growth factor B isoform (*VEGFB*) were upregulated in the presence of 4 or 8 mM Mg. However, under 20% O_2, these increases were reversed into downregulation already with 2 mM Mg. Under 5% O_2, Mg degradation products had no influence on the expression of *PDGFA* and *TIMP1*, while under 20% O_2, the expression of *PDGFA* was statistically

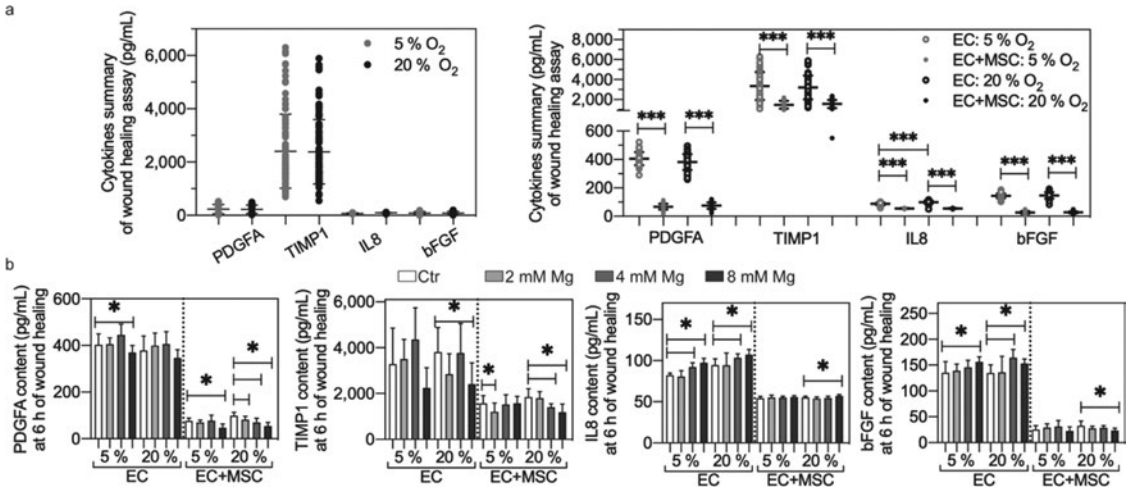

Figure 3. Quantification of cytokines during wound healing. Data (collected from two technical replicates of two independent experiments from cells of three donors; $n = 12$) are represented as arithmetic mean ± standard deviation. (a) To emphasize the effect of oxygen content on cytokine production, different Mg treatments and mono /coculture conditions were merged (left chart). Similarly, to accentuate the effect of mono / coculture conditions on cytokines production, different Mg treatments were merged (right chart). (b) Levels of cytokines under different Mg concentrations, oxygen content, and mono/coculture settings. Significances were investigated by t test or ANOVA and indicated by an asterisk (α = 0.05, $^{*}P \leq 0.05$, $^{**}P \leq 0.01$, and $^{***}P \leq 0.001$).

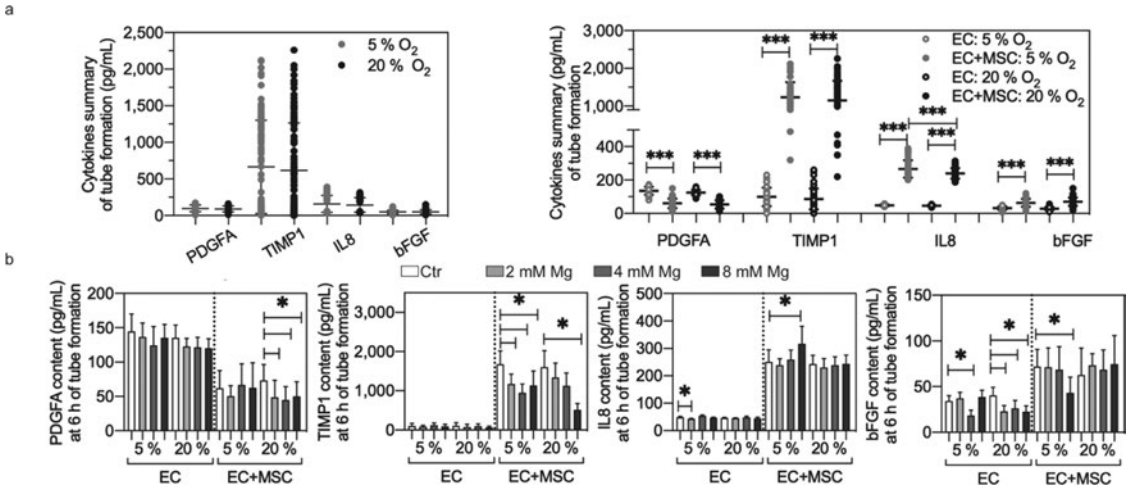

Figure 4. Quantification of cytokines during tube formation. Data (collected from two technical replicates of two independent experiments from cells of three donors; $n = 12$) are represented as arithmetic mean ± standard deviation. (a) To emphasize the effect of oxygen content on cytokine production, different Mg treatments and mono /coculture conditions were merged (left chart). Similarly, to accentuate the effect of mono/ coculture conditions on cytokine production, different Mg treatments were merged (right chart). (b) Levels of cytokines under different Mg concentrations, oxygen content, and mono /coculture settings. Significances were investigated by t test or ANOVA and indicated by an asterisk (α = 0.05, $^{*}P \leq 0.05$, $^{**}P \leq 0.01$, and $^{***}P \leq 0.001$).

upregulated by 8 mM Mg. In wound healing under 5% O_2, *ANG*, hypoxia inducible factor type 1A (*HIF1A*), *IL8*, *TIMP1*, and *VEGFB* expressions in MSCs were not influenced by Mg degradation products. Only *PDGFA* expression was remarkably downregulated with 4 and 8 mM Mg.

During the tube formation of ECs, the gene expressions measured in MSCs were significantly upregulated by Mg under 5% (up to hundreds of times higher than the expressions under 20% O_2). However, the regulation folds between oxygen conditions in ECs were at most 10 times different. Under 5% O_2, *VEGFB* and *TIMP1* in MSCs were remarkably upregulated when cultured with 4 and 8 mM Mg. However, the expression of other MSC genes presented similar U shaped curves. Significantly downregulated *ANG* and *HIF1A* were observed with 2 mM Mg but became upregulated with increased Mg content. Likely, *IL8* and *PDGFA* expressions were decreased (not statistically) under 5% O_2 with 2 and 4 mM Mg. Notably, all investigated genes of MSCs were constantly uninfluenced with up to 8 mM Mg at 20% O_2. In ECs at both 5 and 20% O_2, *ANG*, *TIMP1*, and *VEGFB186* expressions were not regulated after Mg degradation product treatments. Under 5% O_2, obvious upregulation of *HIF1A* as well as *PDGFA* was observed with 8 or 4 mM Mg. However, at 20% O_2, only *HIF1A* was significantly downregulated (2 and 8 mM Mg), while *IL8* and *PDGFA* expressions remained unchanged.

Direct Coculture (Transdifferentiation and Proliferation). Considering heterotypic contact[16] and the high TGFb1 level in direct coculture (Figure 6a), the transdifferentiation potential of MSCs was only investigated when MSCs and ECs were cocultured as a cell mixture. Interestingly, during the coculture

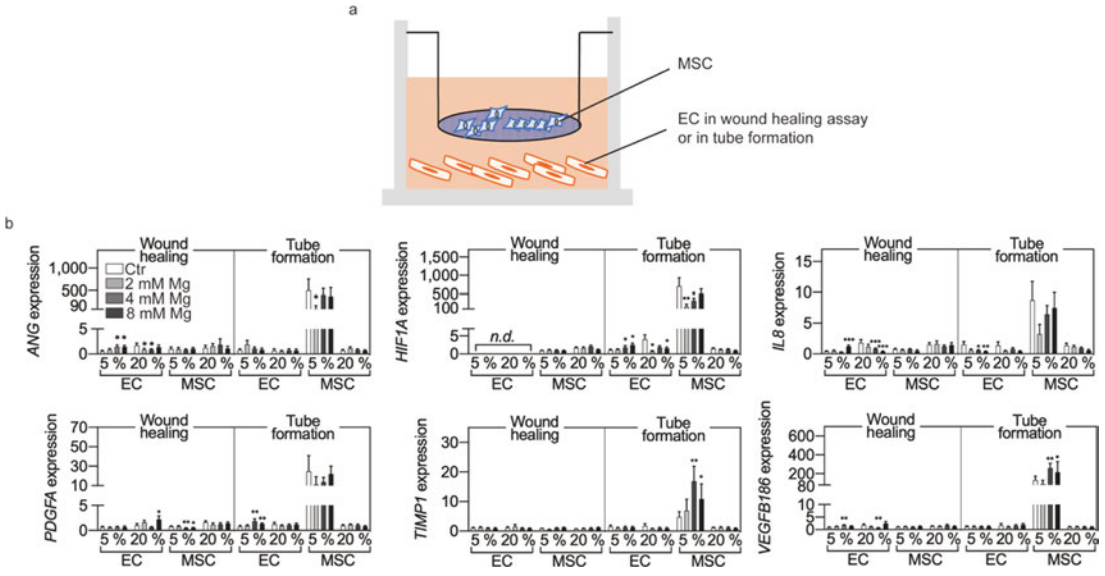

Figure 5. Gene expression of MSCs and ECs during wound healing assay. Data (collected from two technical replicates of two independent experiments from cells of three donors; $n = 12$) are represented as arithmetic mean ± standard deviation. (a) MSCs and ECs were collected separately from transwell inserts and bottom chambers, respectively. (b) Gene expression was investigated by RT qPCR. Significance between treatments and controls were tested *via* one way ANOVA and indicated by an asterisk ($\alpha = 0.05$, $^{*}P \leq 0.05$, $^{**}P \leq 0.01$, and $^{***}P \leq 0.001$).

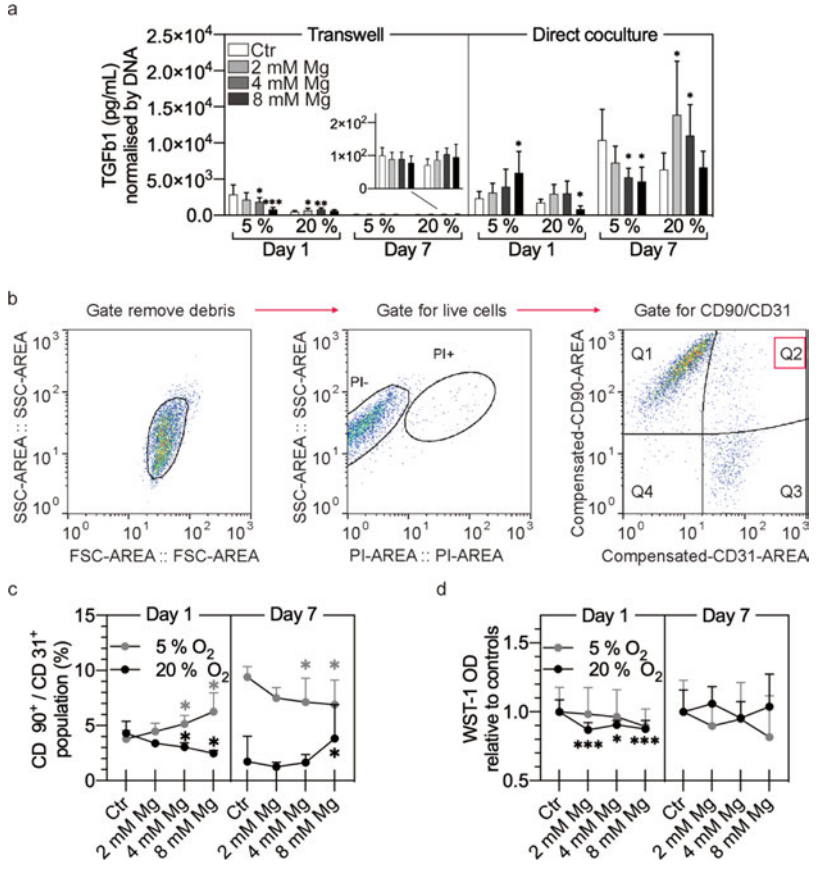

Figure 6. Proliferation and transdifferentiation of MSCs and ECs in coculture. (a) TGFb1 level. (b) Gating procedure and (c) results of flow cytometry. (d) WST 1 at day 1 and 7. Data (collected from two technical replicates of two independent experiments from cells of three donors; $n = 12$) are represented as arithmetic mean ± standard deviation. Significances between Mg treatments and controls were tested *via* one way ANOVA and indicated by an asterisk ($\alpha = 0.05$, $^{*}P \leq 0.05$, and $^{***}P \leq 0.001$).

of MSCs and tube formatting ECs, we observed some upregulation of morphogenesis genes in MSCs (Supporting Information S5) under hypoxic conditions. In addition, only in hypoxia, collagen type I α 1 chain (*COL1A1*), *bFGF*, and fibronectin (*FN1*) were significantly downregulated by 2 or 4 mM Mg. Therefore, we hypothesized that MSCs experienced

phenotype transition during the direct coculture, which could depend on oxygen and be monitored by the double positive CD 90 and 31 using flow cytometry (Figure 6b,c). The proliferation of the MSC−EC mixture was quantified using WST 1 colorimetric assay (Figure 6d).

At day 1 of direct coculture, and compared to the respective controls, the level of TGFb1 in the presence of 8 mM Mg was significantly raised under 5% O_2 but reduced under 20% O_2. At day 7, decreased TGFb1 was observed with 4 and 8 mM Mg under 5% O_2 but increased with 2 and 4 mM Mg under 20% O_2. The percent of double positive events (CD 90^+/CD 31^+) was around 4% for controls at day 1. Similarly, the CD 90^+/CD 31^+ was significantly increased under 5% O_2 but decreased at 20% O_2 with increasing Mg doses (both statistically significant with 4 and 8 mM Mg). On the 7th day, the CD 90^+/CD 31^+ at 5% O_2 was 10% without Mg treatment and started to decrease in the presence of 4 and 8 mM Mg. Under 20% O_2, the CD 90^+/CD 31^+ percent was below 2.5 in controls as well as in the presence of 2 and 4 mM Mg but significantly increased with 8 mM Mg. Mock flow cytometry dot plots are presented in Supporting Information S6. At day 1, the WST 1 OD was shown to be decreased (not statistically significant) with 8 mM Mg under 5% O_2, while significantly decreased with up to 8 mM Mg under 20% O_2. On the 7th day, WST 1 OD was not influenced by Mg under both 5 and 20% O_2.

DISCUSSION

While oxygen concentration variation during metal implant corrosion is not new, observation indicates that degradable materials can make complex the oxygen context because of their local corrosion.[31] Furthermore, emerging results convey the regulatory role of Mg based materials in the activities of ECs, highlighting the therapeutical opportunities of this biomaterials for endovascular therapy. Furthermore, MSCs can promote endothelial migration and neoangiogenesis and induce paracrine secretion.[42−44] Thus, we hypothesis synergistic or nuancing effects of Mg degradation products and oxygen content (corrosion or tissue damage induced) on the MSC influenced endothelial migration and differentiation.

Angiogenesis begins with EC activation from pre existing vasculature and requires participation of specific signaling pathways that enable EC departure and further morphogenesis. The understanding of this mechanism has a high scientific and clinical value. Under hypoxic conditions, the Mg degradation products alone could not induce the EC migration. However, with addition of MSCs, Mg degradation products had a positive influence on EC migration. No matter under normoxia or hypoxia, MSC coculture reduces the EC migration and differentiation when Mg degradation products were present. Therefore, decreased migration is assumed in higher concentrations of Mg degradation products during early corrosion. The comparison between monoculture and coculture indicates the therapeutic potential of MSCs, which release factors modulating migration, inflammation, and thrombosis. PDGF, bFGF, IL8, and TIMP1 are well known MSC tropic factors regulating EC migration and angiogenesis.[45] The PDGF and bFGF, as two potent mitogens, have been applied as therapeutic genes or cytokines for their synergistic effect on MSC proliferation and migration as well as angiogenesis.[46,47] Mg deficiency is believed to induce PDGF secretion,[21] which can be attenuated by extracellular Mg ions.[48] FGF signaling and bFGF were demonstrated to have also a role in bone regeneration of rat calvarial defects.[49] Affinity of bFGF to its receptor is modulated by extracellular Mg.[50] As chemotactic cytokine, IL8 production was proved to be influenced by the Mg ions.[51] The TIMPs proteolytically cleave and inactivate MMP activity and therefore mediate the extracellular matrix (ECM) reorganization during migration. Mg treatments attenuate the TIMP level in many inflammatory symptoms.[52]

The hypoxia upregulated genes, such as *ANG*, *IL8*, and *VEGFB186*, suggested that ECs are more likely to migrate and proliferate at the hypoxic area. ANG can regulate the proliferation and attenuate inflammation *via* counteracting IL8.[53] IL8 exerts its activity *via* VEGF pathways. VEGF is a major signaling pathway for EC activation.[54] Additionally, hypoxia can also stimulate HIF1A and PDGFA, which can trigger many subsequent pathways for migration and differentiation.[54,55] Therefore, more re endothelialization can be expected on the hypoxic interface of endothelium. On the contrary, both migration and differentiation of ECs tend to be downregulated under normoxia. Hypoxia can modulate MSC proliferation and differentiation through ANG, bFGF, and PDGFA.[56−59] Additionally, hypoxia decreases factors relative to ECM synthesis and interaction, that is, BMPs, FN1, COL1A1, BMP4, and BMPR1A.[60−63] On the contrary, normoxia tends to stabilize the expression of selected genes in MSCs. Therefore, more undifferentiated MSCs could be expected at the hypoxic site of lesions or materials, in which the oxygen may promote the stemness and secretion of angiogenic factors of MSCs.[64]

Transdifferentiation, also known as lineage reprogramming, is a critical step to restore the endothelium post stenting (re endothelialization) and the tissue development. MSCs can be differentiated into ECs (mesenchymal−endothelial transition−MET) *in vitro*,[65] while ECs can lose their specific markers and acquire a mesenchymal phenotype[66] (endothelial−mesenchymal transition−EndoMT). The TGFb pathway is reported to mediate this transition by supporting EndMT[66] but inhibiting MET.[67] TGFb can inhibit the EC growth of different cell sources[68] by altering the cellular response to growth stimulatory factors. HIF1A is the main cellular response induced by hypoxia exposure and synergistically acts with TGFb.[69] The present results suggest that the MSC−EC transdifferentiation is reciprocally regulated by Mg degradation products in the two different oxygen conditions. Based on a former study, the reciprocal effects of Mg could depend on the fact that Mg downregulates HIFs at 5% but upregulates them under 20% O_2.[25] As EndoMT contributes to a multitude of diseases while MET can enhance the tissue repair, modulation of these signaling pathways may prove to be an effective target for therapeutic treatment.[18,70] Thus, environmental oxygen and the interaction with Mg materials could be a way for improving cellular transdifferentiation of the unideal somatic cells and stem cells.

CONCLUSIONS

We investigated the oxygen contents and biochemical environments vascularization could be exposed to during Mg based biomaterial degradation, paracrine secretion, and heterotypic contact of MSCs. Our results consolidate the suitability of Mg based absorbable materials for therapeutic vascularization strategies and tissue engineering. Oxygen concentration as well as degradation rate of resolvable metal based biomaterials could be essential parameters to be monitored or tailored in order to modulate the distribution

and fate of exogenously delivered MSCs and to tune the regeneration of tissues.

AUTHOR INFORMATION

Corresponding Author

Bérengère J. C. Luthringer Feyerabend − *Institute of Materials Research, Division for Metallic Biomaterials, Helmholtz Zentrum Geesthacht (HZG), Geesthacht 21502, Germany;* orcid.org/0000 0002 8248 6715; Phone: +49 (0)4152 87 1292; Email: Berengere.Luthringer@hzg.de; Fax: +49 (0)4152 87 2595

Authors

Lei Xu − *Institute of Materials Research, Division for Metallic Biomaterials, Helmholtz Zentrum Geesthacht (HZG), Geesthacht 21502, Germany;* orcid.org/0000 0002 0512 4796

Regine Willumeit Römer − *Institute of Materials Research, Division for Metallic Biomaterials, Helmholtz Zentrum Geesthacht (HZG), Geesthacht 21502, Germany*

Author Contributions

All authors have contributed to the study conception and design. The manuscript was written through contributions of all authors. All authors have seen and approved the manuscript being submitted. L.X. performed material preparation, experiments, data collection, and analysis.

Notes

The authors declare no competing financial interest.

ACKNOWLEDGMENTS

L.X. was funded by China Scholarship Council (CSC, 201508110199). We appreciate Prof. Dr. Volker Ragosch, from Asklepios Klinik Altona, Hamburg, Germany, for the umbilical cord.

REFERENCES

(1) Luthringer, B. J. C.; Feyerabend, F.; Willumeit Römer, R. Magnesium based implants: a mini review. *Magnesium Res.* **2014**, *27*, 142−154.

(2) Zhang, C.; Wen, T. H.; Razak, K. A.; Lin, J.; Xu, C.; Seo, C.; Villafana, E.; Jimenez, H.; Liu, H. Magnesium based biodegradable microelectrodes for neural recording. *Mater. Sci. Eng., C* **2020**, *110*, 110614.

(3) Hopkins, T. M.; Little, K. J.; Vennemeyer, J. J.; Triozzi, J. L.; Turgeon, M. K.; Heilman, A. M.; Minteer, D.; Marra, K.; Hom, D. B.; Pixley, S. K. Short and long gap peripheral nerve repair with magnesium metal filaments. *J. Biomed. Mater. Res., Part A* **2017**, *105*, 3148−3158.

(4) Qiao, S.; Wang, Y.; Zan, R.; Wu, H.; Sun, Y.; Peng, H.; Zhang, R.; Song, Y.; Ni, J.; Zhang, S.; Zhang, X. Biodegradable Mg Implants Suppress the Growth of Ovarian Tumor. *ACS Biomater. Sci. Eng.* **2020**, *6*, 1755−1763.

(5) Song, G.; Nguyen, D. T.; Pietramaggiori, G.; Scherer, S.; Chen, B.; Zhan, Q.; Ogawa, R.; Yannas, I. V.; Wagers, A. J.; Orgill, D. P.; Murphy, G. F. Use of the parabiotic model in studies of cutaneous wound healing to define the participation of circulating cells. *Wound Repair Regen.* **2010**, *18*, 426−432.

(6) Ullah, I.; Subbarao, R. B.; Rho, G. J. Human mesenchymal stem cells current trends and future prospective. *Biosci. Rep.* **2015**, *35*, No. e00191.

(7) Melchiorri, A. J.; Nguyen, B. N. B.; Fisher, J. P. Mesenchymal stem cells: roles and relationships in vascularization. *Tissue Eng., Part B* **2014**, *20*, 218−228.

(8) Pankajakshan, D.; Agrawal, D. K. Mesenchymal Stem Cell Paracrine Factors in Vascular Repair and Regeneration. *J. Biomed. Technol. Res.* **2014**, *1*, 9.

(9) Lieu, C.; Heymach, J.; Overman, M.; Tran, H.; Kopetz, S. Beyond VEGF: inhibition of the fibroblast growth factor pathway and antiangiogenesis. *Clin. Cancer Res.* **2011**, *17*, 6130−6139.

(10) Wang, J.; Wang, Y.; Wang, S.; Cai, J.; Shi, J.; Sui, X.; Cao, Y.; Huang, W.; Chen, X.; Cai, Z.; Li, H.; Bardeesi, A. S. A.; Zhang, B.; Liu, M.; Song, W.; Wang, M.; Xiang, A. P. Bone marrow derived mesenchymal stem cell secreted IL 8 promotes the angiogenesis and growth of colorectal cancer. *Oncotarget* **2015**, *6*, 42825−42837.

(11) Benn, A.; Bredow, C.; Casanova, I.; Vukičević, S.; Knaus, P. VE cadherin facilitates BMP induced endothelial cell permeability and signaling. *J. Cell Sci.* **2016**, *129*, 206−218.

(12) Arpino, V.; Mehta, S.; Wang, L.; Bird, R.; Rohan, M.; Pape, C.; Gill, S. E. Tissue inhibitor of metalloproteinases 3 dependent microvascular endothelial cell barrier function is disrupted under septic conditions. *Am. J. Physiol. Heart Circ. Physiol.* **2016**, *310*, H1455−H1467.

(13) Zielińska, K. A.; Van Moortel, L.; Opdenakker, G.; De Bosscher, K.; Van den Steen, P. E. Endothelial Response to Glucocorticoids in Inflammatory Diseases. *Front. Immunol.* **2016**, *7*, 592.

(14) Boomsma, R. A.; Geenen, D. L. Mesenchymal Stem Cells Secrete Multiple Cytokines That Promote Angiogenesis and Have Contrasting Effects on Chemotaxis and Apoptosis. *PLoS One* **2012**, *7*, No. e35685.

(15) Ho, I. A. W.; Toh, H. C.; Ng, W. H.; Teo, Y. L.; Guo, C. M.; Hui, K. M.; Lam, P. Y. P. Human bone marrow derived mesenchymal stem cells suppress human glioma growth through inhibition of angiogenesis. *Stem Cell.* **2013**, *31*, 146−155.

(16) Voura, E. B.; Sandig, M.; Siu, C. H. Cell cell interactions during transendothelial migration of tumor cells. *Microsc. Res. Tech.* **1998**, *43*, 265−275.

(17) Pedersen, T. O.; Blois, A. L.; Xue, Y.; Xing, Z.; Sun, Y.; Finne Wistrand, A.; Lorens, J. B.; Fristad, I.; Leknes, K. N.; Mustafa, K. Mesenchymal stem cells induce endothelial cell quiescence and promote capillary formation. *Stem Cell Res. Ther.* **2014**, *5*, 23.

(18) Ubil, E.; Duan, J.; Pillai, I. C. L.; Rosa Garrido, M.; Wu, Y.; Bargiacchi, F.; Lu, Y.; Stanbouly, S.; Huang, J.; Rojas, M.; Vondriska, T. M.; Stefani, E.; Deb, A. Mesenchymal−endothelial transition contributes to cardiac neovascularization. *Nature* **2014**, *514*, 585.

(19) Zhu, D.; You, J.; Zhao, N.; Xu, H. Magnesium Regulates Endothelial Barrier Functions through TRPM7, MagT1, and S1P1. *Adv. Sci.* **2019**, *6*, 1901166.

(20) Baldoli, E.; Maier, J. A. M. Silencing TRPM7 mimics the effects of magnesium deficiency in human microvascular endothelial cells. *Angiogenesis* **2012**, *15*, 47−57.

(21) Ferrè, S.; Baldoli, E.; Leidi, M.; Maier, J. A. M. Magnesium deficiency promotes a pro atherogenic phenotype in cultured human endothelial cells via activation of NFkB. *Biochim. Biophys. Acta, Mol. Basis Dis.* **2010**, *1802*, 952−958.

(22) Maier, J. A. M.; Malpuech Brugère, C.; Zimowska, W.; Rayssiguier, Y.; Mazur, A. Low magnesium promotes endothelial

cell dysfunction: implications for atherosclerosis, inflammation and thrombosis. *Biochim. Biophys. Acta, Mol. Basis Dis.* **2004**, *1689*, 13−21.
(23) Bernardini, D.; Nasulewic, A.; Mazur, A.; Maier, J. A. Magnesium and microvascular endothelial cells: a role in inflammation and angiogenesis. *Front. Biosci.* **2005**, *10*, 1177−1182.
(24) Darooghegi Mofrad, M.; Djafarian, K.; Mozaffari, H.; Shab Bidar, S. Effect of magnesium supplementation on endothelial function: A systematic review and meta analysis of randomized controlled trials. *Atherosclerosis* **2018**, *273*, 98−105.
(25) Xu, L.; Willumeit Römer, R.; Luthringer Feyerabend, B. J. C. Effect of magnesium degradation products and hypoxia on the angiogenesis of human umbilical vein endothelial cells. *Acta Biomater.* **2019**, *98*, 269−283.
(26) Zhao, D.; Huang, S.; Lu, F.; Wang, B.; Yang, L.; Qin, L.; Yang, K.; Li, Y.; Li, W.; Wang, W.; Tian, S.; Zhang, X.; Gao, W.; Wang, Z.; Zhang, Y.; Xie, X.; Wang, J.; Li, J. Vascularized bone grafting fixed by biodegradable magnesium screw for treating osteonecrosis of the femoral head. *Biomaterials* **2016**, *81*, 84−92.
(27) da Silva Lima, F.; da Rocha Romero, A. B.; Hastreiter, A.; Nogueira Pedro, A.; Makiyama, E.; Colli, C.; Fock, R. A. An insight into the role of magnesium in the immunomodulatory properties of mesenchymal stem cells. *J. Nutr. Biochem.* **2018**, *55*, 200−208.
(28) Luthringer, B. J. C.; Willumeit Römer, R. Effects of magnesium degradation products on mesenchymal stem cell fate and osteoblastogenesis. *Gene* **2016**, *575*, 9−20.
(29) Yoshizawa, S.; Brown, A.; Barchowsky, A.; Sfeir, C. Role of magnesium ions on osteogenic response in bone marrow stromal cells. *Connect. Tissue Res.* **2014**, *55*, 155−159.
(30) Zhao, N.; Zhu, D. Endothelial responses of magnesium and other alloying elements in magnesium based stent materials. *Metallomics* **2015**, *7*, 118−128.
(31) Silva, E. L.; Lamaka, S. V.; Mei, D.; Zheludkevich, M. L. The Reduction of Dissolved Oxygen During Magnesium Corrosion. *ChemistryOpen* **2018**, *7*, 664−668.
(32) Haque, N.; Rahman, M. T.; Abu Kasim, N. H.; Alabsi, A. M. Hypoxic culture conditions as a solution for mesenchymal stem cell based regenerative therapy. *Sci. World J.* **2013**, *2013*, 1.
(33) Carreau, A.; Hafny Rahbi, B. E.; Matejuk, A.; Grillon, C.; Kieda, C. Why is the partial oxygen pressure of human tissues a crucial parameter? Small molecules and hypoxia. *J. Cell. Mol. Med.* **2011**, *15*, 1239−1253.
(34) Lu, C.; Rollins, M.; Hou, H.; Swartz, H. M.; Hopf, H.; Miclau, T.; Marcucio, R. S. Tibial fracture decreases oxygen levels at the site of injury. *Iowa Orthop. J.* **2008**, *28*, 14−21.
(35) Han, Y. S.; Lee, J. H.; Yoon, Y. M.; Yun, C. W.; Noh, H.; Lee, S. H. Hypoxia induced expression of cellular prion protein improves the therapeutic potential of mesenchymal stem cells. *Cell Death Dis.* **2016**, *7*, No. e2395.
(36) Holzwarth, C.; Vaegler, M.; Gieseke, F.; Pfister, S. M.; Handgretinger, R.; Kerst, G.; Müller, I. Low physiologic oxygen tensions reduce proliferation and differentiation of human multipotent mesenchymal stromal cells. *BMC Cell Biol.* **2010**, *11*, 11.
(37) Jones, C. I., 3rd; Han, Z.; Presley, T.; Varadharaj, S.; Zweier, J. L.; Ilangovan, G.; Alevriadou, B. R. Endothelial cell respiration is affected by the oxygen tension during shear exposure: role of mitochondrial peroxynitrite. *Am. J. Physiol. Cell Physiol.* **2008**, *295*, C180−C191.
(38) Faulkner, A.; Purcell, R.; Hibbert, A.; Latham, S.; Thomson, S.; Hall, W. L.; Wheeler Jones, C.; Bishop Bailey, D. A thin layer angiogenesis assay: a modified basement matrix assay for assessment of endothelial cell differentiation. *BMC Cell Biol.* **2014**, *15*, 41.
(39) Luthringer, B. J. C.; Ali, F.; Akaichi, H.; Feyerabend, F.; Ebel, T.; Willumeit, R. Production, characterisation, and cytocompatibility of porous titanium based particulate scaffolds. *J. Mater. Sci.: Mater. Med.* **2013**, *24*, 2337−2358.
(40) Xu, L.; Willumeit Römer, R.; Luthringer Feyerabend, B. Hypoxia influences the effects of magnesium degradation products on the interactions between endothelial and mesenchymal stem cells. *Acta Biomater.* **2020**, *101*, 624−636.
(41) Bates, M. K. Culturing Cells Under Hypoxic Conditions for Biologically Relevant Results. https://www.americanlaboratory.com/913 Technical Articles/123131 Culturing Cells Under Hypoxic Conditions for Biologically Relevant Results/ (accessed 09.01.2021).
(42) Al Khaldi, A.; Eliopoulos, N.; Martineau, D.; Lejeune, L.; Lachapelle, K.; Galipeau, J. Postnatal bone marrow stromal cells elicit a potent VEGF dependent neoangiogenic response in vivo. *Gene Ther.* **2003**, *10*, 621−629.
(43) Gruber, R.; Kandler, B.; Holzmann, P.; Vögele Kadletz, M.; Losert, U.; Fischer, M. B.; Watzek, G. Bone marrow stromal cells can provide a local environment that favors migration and formation of tubular structures of endothelial cells. *Tissue Eng.* **2005**, *11*, 896−903.
(44) Hsieh, J. Y.; Wang, H. W.; Chang, S. J.; Liao, K. H.; Lee, I. H.; Lin, W. S.; Wu, C. H.; Lin, W. Y.; Cheng, S. M. Mesenchymal stem cells from human umbilical cord express preferentially secreted factors related to neuroprotection, neurogenesis, and angiogenesis. *PLoS One* **2013**, *8*, No. e72604.
(45) Chen, J.; Liu, Z.; Hong, M. M.; Zhang, H.; Chen, C.; Xiao, M.; Wang, J.; Yao, F.; Ba, M.; Liu, J.; Guo, Z. K.; Zhong, J. Proangiogenic Compositions of Microvesicles Derived from Human Umbilical Cord Mesenchymal Stem Cells. *PLoS One* **2014**, *9*, No. e115316.
(46) Chen, W.; Baylink, D. J.; Brier Jones, J.; Neises, A.; Kiroyan, J. B.; Rundle, C. H.; Lau, K. H. W.; Zhang, X. B. PDGFB based stem cell gene therapy increases bone strength in the mouse. *Proc. Natl. Acad. Sci. U.S.A.* **2015**, *112*, E3893−E3900.
(47) Stratman, A. N.; Schwindt, A. E.; Malotte, K. M.; Davis, G. E. Endothelial derived PDGF BB and HB EGF coordinately regulate pericyte recruitment during vasculogenic tube assembly and stabilization. *Blood* **2010**, *116*, 4720−4730.
(48) Kawano, H.; Yokoyama, S.; Smith, T. L.; Nishida, H. I.; Taguchi, T.; Kummerow, F. A. Effect of magnesium on secretion of platelet derived growth factor by cultured human umbilical arterial endothelial cells. *Magnesium Res.* **1995**, *8*, 137−144.
(49) Chen, M.; Song, K.; Rao, N.; Huang, M.; Huang, Z.; Cao, Y. Roles of exogenously regulated bFGF expression in angiogenesis and bone regeneration in rat calvarial defects. *Int. J. Mol. Med.* **2011**, *27*, 545−553.
(50) Baird, A. Potential mechanisms regulating the extracellular activities of basic fibroblast growth factor (FGF 2). *Mol. Reprod. Dev.* **1994**, *39*, 43−48.
(51) Rochelson, B.; Dowling, O.; Schwartz, N.; Metz, C. N. Magnesium sulfate suppresses inflammatory responses by human umbilical vein endothelial cells (HuVECs) through the NFκB pathway. *J. Reprod. Immunol.* **2007**, *73*, 101−107.
(52) Asai, T.; Nakatani, T.; Yamanaka, S.; Tamada, S.; Kishimoto, T.; Tashiro, K.; Nakao, T.; Okamura, M.; Kim, S.; Iwao, H.; Miura, K. Magnesium supplementation prevents experimental chronic cyclosporine a nephrotoxicity via renin angiotensin system independent mechanism. *Transplantation* **2002**, *74*, 784−791.
(53) Pizurki, L.; Zhou, Z.; Glynos, K.; Roussos, C.; Papapetropoulos, A. Angiopoietin 1 inhibits endothelial permeability, neutrophil adherence and IL 8 production. *Br. J. Pharmacol.* **2003**, *139*, 329−336.
(54) Feng, N.; Chen, H.; Fu, S.; Bian, Z.; Lin, X.; Yang, L.; Gao, Y.; Fang, J.; Ge, Z. HIF 1alpha and HIF 2alpha induced angiogenesis in gastrointestinal vascular malformation and reversed by thalidomide. *Sci. Rep.* **2016**, *6*, 27280.
(55) Lee, Y. H.; Bae, H. C.; Noh, K. H.; Song, K. H.; Ye, S. k.; Mao, C. P.; Lee, K. M.; Wu, T. C.; Kim, T. W. Gain of HIF 1alpha under normoxia in cancer mediates immune adaptation through the AKT/ERK and VEGFA axes. *Clin. Cancer Res.* **2015**, *21*, 1438−1446.
(56) Ahn, H. J.; Lee, W. J.; Kwack, K.; Kwon, Y. D. FGF2 stimulates the proliferation of human mesenchymal stem cells through the transient activation of JNK signaling. *FEBS Lett.* **2009**, *583*, 2922−2926.
(57) Donovan, J.; Abraham, D.; Norman, J. Platelet derived growth factor signaling in mesenchymal cells. *Front. Biosci.* **2013**, *18*, 106−119.

(58) Lai, W. T.; Krishnappa, V.; Phinney, D. G. Fibroblast growth factor 2 (Fgf2) inhibits differentiation of mesenchymal stem cells by inducing Twist2 and Spry4, blocking extracellular regulated kinase activation, and altering Fgf receptor expression levels. *Stem Cell.* **2011**, *29*, 1102−1111.
(59) Liu, X. H.; Bai, C. G.; Xu, Z. Y.; Huang, S. D.; Yuan, Y.; Gong, D. J.; Zhang, J. R. Therapeutic potential of angiogenin modified mesenchymal stem cells: angiogenin improves mesenchymal stem cells survival under hypoxia and enhances vasculogenesis in myocardial infarction. *Microvasc. Res.* **2008**, *76*, 23−30.
(60) Beederman, M.; Lamplot, J. D.; Nan, G.; Wang, J.; Liu, X.; Yin, L.; Li, R.; Shui, W.; Zhang, H.; Kim, S. H.; Zhang, W.; Zhang, J.; Kong, Y.; Denduluri, S.; Rogers, M. R.; Pratt, A.; Haydon, R. C.; Luu, H. H.; Angeles, J.; Shi, L. L.; He, T. C. BMP signaling in mesenchymal stem cell differentiation and bone formation. *J. Biomed. Sci. Eng.* **2013**, *06*, 32−52.
(61) Biswas, S.; Li, P.; Wu, H.; Shafiquzzaman, M.; Murakami, S.; Schneider, M. D.; Mishina, Y.; Li, B.; Li, J. BMPRIA is required for osteogenic differentiation and RANKL expression in adult bone marrow mesenchymal stromal cells. *Sci. Rep.* **2018**, *8*, 8475.
(62) Clements, L. E.; Garvican, E. R.; Dudhia, J.; Smith, R. K. W. Modulation of mesenchymal stem cell genotype and phenotype by extracellular matrix proteins. *Connect. Tissue Res.* **2016**, *57*, 443−453.
(63) Singh, P.; Schwarzbauer, J. E. Fibronectin and stem cell differentiation lessons from chondrogenesis. *J. Cell Sci.* **2012**, *125*, 3703−3712.
(64) Sharma, D.; Chica, J.; Zhao, F. Mesenchymal stem cells for pre vascularization of engineered tissues. *J. Stem Cell Res. Ther.* **2018**, *4*, 41.
(65) Oswald, J.; Boxberger, S.; Jørgensen, B.; Feldmann, S.; Ehninger, G.; Bornhäuser, M.; Werner, C. Mesenchymal stem cells can be differentiated into endothelial cells in vitro. *Stem Cell.* **2004**, *22*, 377−384.
(66) Piera Velazquez, S.; Li, Z.; Jimenez, S. A. Role of endothelial mesenchymal transition (EndoMT) in the pathogenesis of fibrotic disorders. *Am. J. Pathol.* **2011**, *179*, 1074−1080.
(67) Wang, M. K.; Sun, H. Q.; Xiang, Y. C.; Jiang, F.; Su, Y. P.; Zou, Z. M. Different roles of TGF beta in the multi lineage differentiation of stem cells. *World J. Stem Cell.* **2012**, *4*, 28−34.
(68) Hirschi, K. K.; Rohovsky, S. A.; D'Amore, P. A. PDGF, TGF β, and heterotypic cell−cell interactions mediate endothelial cell−induced recruitment of 10T1/2 cells and their differentiation to a smooth muscle fate. *J. Cell Biol.* **1998**, *141*, 805−814.
(69) Mingyuan, X.; Qianqian, P.; Shengquan, X.; Chenyi, Y.; Rui, L.; Yichen, S.; Jinghong, X. Hypoxia inducible factor 1alpha activates transforming growth factor beta1/Smad signaling and increases collagen deposition in dermal fibroblasts. *Oncotarget* **2018**, *9*, 3188−3197.
(70) Man, S.; Sanchez Duffhues, G.; Ten Dijke, P.; Baker, D. The therapeutic potential of targeting the endothelial to mesenchymal transition. *Angiogenesis* **2019**, *22*, 3−13.